



The Unusual Homodimer of a Heme-Copper Terminal Oxidase Allows Itself to Utilize Two Electron Donors

Guoliang Zhu[†], Hui Zeng^{†,*}, Shuangbo Zhang[†], Jana Juli, Linhua Tai, Danyang Zhang, Xiaoyun Pang, Yan Zhang, Sin Man Lam, Yun Zhu,^{*} Guohong Peng,^{*} Hartmut Michel,^{*} and Fei Sun^{*}

Abstract: The heme-copper oxidase superfamily comprises cytochrome *c* and ubiquinol oxidases. These enzymes catalyze the transfer of electrons from different electron donors onto molecular oxygen. A B-family cytochrome *c* oxidase from the hyperthermophilic bacterium *Aquifex aeolicus* was discovered previously to be able to use both cytochrome *c* and naphthoquinol as electron donors. Its molecular mechanism as well as the evolutionary significance are yet unknown. Here we solved its 3.4 Å resolution electron cryo-microscopic structure and discovered a novel dimeric structure mediated by subunit I (CoxA2) that would be essential for naphthoquinol binding and oxidation. The unique structural features in both proton and oxygen pathways suggest an evolutionary adaptation of this oxidase to its hyperthermophilic environment. Our results add a new conceptual understanding of structural variation of cytochrome *c* oxidases in different species.

Introduction

In all respiring organisms electrochemical proton gradients drive the flux of protons back through the membrane via ATP-synthases, which produces adenosine-5'-triphosphate by attaching an inorganic phosphate to adenosine-5'-diphosphate. In aerobic organisms, the electrochemical proton gradient is generated by a series of proton translocation reactions in the respiratory chains. Cytochrome *c* oxidase

(CcO) is the terminal enzyme in the respiratory chains of many aerobic organisms. It is located in the inner membrane of mitochondria and bacteria, and catalyzes the electron transfer from cytochrome *c* to molecular oxygen that is reduced to water. Studies on this integral membrane protein complex revealed that eight protons are taken up from the matrix side of mitochondrial membrane or from the bacterial cytoplasm (N-side), four protons are pumped across the membrane into the intermembrane space of mitochondria or the periplasm of gram-negative bacteria (P-side), while another four protons are used for water formation.^[1]

CcO is a member of the heme- and copper-containing terminal oxidases (HCOs) superfamily,^[2] which also includes ubiquinol oxidases (QOXs), for example, the well-studied cytochrome *bo*₃ from *Escherichia coli* (*E. coli*)^[3] but not the cytochrome *bd* oxidases from the same bacterium.^[4] HCOs are classified into three families, A, B and C, based on their amino acid sequences and proton transfer pathways.^[5] They are multi-subunit complexes, for example, they possess 14 protein subunits in mammalian mitochondria^[6] and 3 subunits in some bacteria.^[7]

The conserved central catalytic subunit I contains two heme groups and a copper atom (Cu_B). The low-spin heme can be a heme *a* or a heme *b* in prokaryotes,^[3,8] whereas only heme *a* has been found in mitochondrial cytochrome *c* oxidases.^[9] The low-spin heme *a* in the A-family CcO from

[*] G. L. Zhu,^[†] S. B. Zhang,^[†] L. H. Tai, D. Y. Zhang, X. Y. Pang, Y. Zhang, Y. Zhu, G. H. Peng, F. Sun
National Key Laboratory of Biomacromolecules, CAS Center for Excellence in Biomacromolecules, Institute of Biophysics, Chinese Academy of Sciences
15 Datun Road, Chaoyang District, Beijing, 100101 (China)
E-mail: zhuyun@ibp.ac.cn
feisun@ibp.ac.cn

H. Zeng,^[†] J. Juli, G. H. Peng, H. Michel
Department of Molecular Membrane Biology,
Max Planck Institute of Biophysics
Max-von Laue-Straße 3, 60438 Frankfurt am Main (Germany)
E-mail: huzeng@biophys.mpg.de
Guohong.Peng@biophys.mpg.de
Hartmut.Michel@biophys.mpg.de

G. L. Zhu,^[†] S. B. Zhang,^[†] L. H. Tai, D. Y. Zhang, Y. Zhu, F. Sun
College of Life Sciences, University of Chinese Academy of Sciences
Beijing, 100049 (China)

F. Sun
Center for Biological Imaging, Institute of Biophysics,
Chinese Academy of Sciences
15 Datun Road, Chaoyang District, Beijing, 100101 (China)

S. M. Lam
LipidALL Technologies Company Limited
Changzhou 213022, Jiangsu Province (China)
and
State Key Laboratory of Molecular Developmental Biology, Institute of Genetics and Developmental Biology,
Chinese Academy of Sciences
No.1 West Beichen Road, Chaoyang District, Beijing, 100101 (China)

[†] These authors contributed equally to this work.

Supporting information and the ORCID identification number(s) for the author(s) of this article can be found under:
<https://doi.org/10.1002/anie.202016785>.

© 2021 The Authors. Angewandte Chemie International Edition published by Wiley-VCH GmbH. This is an open access article under the terms of the Creative Commons Attribution License, which permits use, distribution and reproduction in any medium, provided the original work is properly cited.

Bos taurus (BtCcO)^[9b] and heme *b* in the B-family CcO from *Thermus thermophilus* (TtCcO) accept electrons from Cu_A,^[7] and transfer them to the active site that is formed by the high-spin heme *a*₃ and Cu_B. The low-spin heme *b* in the QOX from *E. coli* directly accepts electrons from ubiquinol and transfers them to the binuclear center that is formed by a high-spin heme *o*₃ and Cu_B.^[10] When the binuclear center becomes doubly reduced, dioxygen binds to the heme iron and is reduced to water. The required protons are provided from the cytoplasmic side.

Subunit I of the CcOs most often contains 12 transmembrane helices (TMHs). An exception is TtCcO whose subunit I possesses 13 transmembrane helices.^[7] Subunit II is well conserved in the A- and B-families with its binuclear Cu_A center located at the P-side and accepting electrons from cytochrome *c*,^[11] whereas in QOXs subunit II contains two TMHs with Cu_A absent.^[10,12] Subunit III is present in mitochondrial and most bacterial HCOs in A-family, and could be fused to subunit I.^[13]

TtCcO is the best studied HCO of the B-family. Its crystal structures in the oxidized state have been reported at resolutions of 2.4 Å^[7] and 1.8 Å,^[14] respectively. Its proton pathway was found to be similar to the K-pathway of A-family CcO.^[15] Differently, compared to the A-family CcO (PdCcO) from *Paracoccus denitrificans* (*P. denitrificans*), subunit II of TtCcO only contains one TMH. The position of the second N-terminal TMH of PdCcO subunit II is occupied by the additional subunit IIa of TtCcO in an opposite orientation.^[7] Although it has been challenged recently,^[16] several studies suggested the efficiency of proton pumping in B-family CcOs ($H^+/e^- = 0.5$)^[17] appears to be lower than that of A-family CcOs ($H^+/e^- = 1$).^[18]

Aquifex aeolicus (*A. aeolicus*) is a hyperthermophilic chemolithoautotrophic bacterium. The cytochrome *c* oxidase from *A. aeolicus*, AaCcO, was previously discovered belonging to B-family HCO, and interestingly could use both cytochrome *c* and ubiquinol as electron donors,^[19] which is a unique feature as a member of B-family HCO. We originally hypothesized it would be caused by formation of supercomplex between AaCcO and complex III, providing additional quinol binding sites to enable its direct oxidation bypass cytochrome *c*. However, by solving the structure of *A. aeolicus* complex III,^[20] we did not find novel structural features to support this hypothesis. In addition, our previous study showed the ubiquinol oxidation activity of the potential supercomplex was insensitive to stigmatellin, the inhibitor of ubiquinol binding of complex III.^[19] Thus, the ubiquinol oxidation activity of the specimen would most likely come from AaCcO itself. It would be the own structural variation of AaCcO to gain the function of additional quinol oxidation.

To gain insights into the molecular mechanism of AaCcO and also to understand how AaCcO adapts its structure to keep stability and activity under hyperthermophilic growth conditions, we purified the AaCcO from native membranes and determined its structure at 3.4 Å resolution by using single-particle electron cryo-microscopy (cryo-EM). We found a dimeric form of AaCcO with a novel binding site of the native quinol (VII-tetrahydromultiprenyl-1,4 naphthoquinone, NQ) at the dimeric interface, which could allow

NQH₂ to be a direct electron donor bypassing cytochrome *c*. Further structure comparisons revealed structural variations of AaCcO to increase structural stability and alter the proton transfer pathway as well as the oxygen diffusion pathway for its adaptation of the hyperthermophilic growth environment.

Results

Overall structure of AaCcO dimer

The AaCcO sample was enriched by anion exchange chromatography and further purified by size-exclusion chromatography, and the fractions showing a dominant homogeneous band around 242 kDa in Blue Native PAGE were used for subsequent cryo-EM experiments (Figure S1). Based on cryo-EM 3D classification using RELION^[21] (Figure S2), we found two well-aligned classes of particles existing in the current purified sample. The first class represents the structure of dimeric complex III reported by us before^[20] and the second represents the structure of dimeric AaCcO. Our substantial image processing does not suggest the existing of any potential supercomplex in this sample. After *in silico* purification, the dimeric AaCcO structure was determined at a final resolution of 3.4 Å according to the gold standard FSC_{0.143} (Fourier Shell Correlation) criterion (Figures S2, S4 and S5; Movie S1). The AaCcO dimer exhibits a C2 symmetry and contains three subunits (Figure 1A), subunit I (CoxA2, 63.9 kDa) with the heme *b* and the heme *a*₃/Cu_B active site, subunit II (CoxB2, 16.8 kDa) with the Cu_A center, and subunit IIa (5.2 kDa) (Figure S1). It has dimensions of 84.7 Å in height and 107.7 Å in length. The length of the AaCcO monomer is 55.0 Å. The cofactors Cu_A, Cu_B, heme *a*₃ and heme *b* are well resolved (Figure 1B and Figure S4) with the edge-to-edge distance between Cu_A and heme *b* Fe 15.4 Å, and the edge-to-edge distances from heme *b* to heme

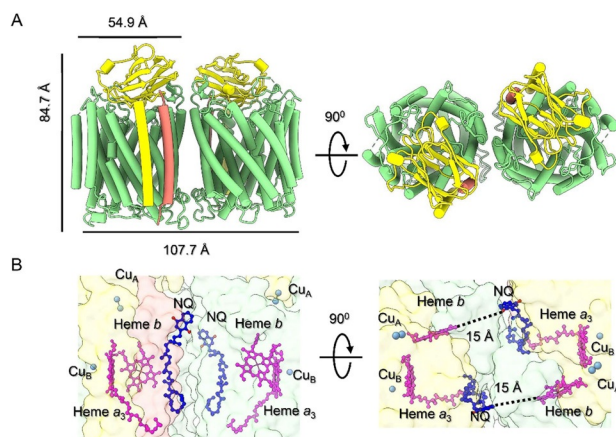


Figure 1. Overall structure of AaCcO. A) The protein structure of AaCcO is shown in two different views, with the dimensions indicated. The subunits CoxA2, CoxB2, and IIa are colored in green, yellow, and orange, respectively. B) The cofactors and quinols (NQs) are shown as stick representations. The color scheme of subunits CoxA2, CoxB2, and IIa is the same as in (A). The edge-to-edge distances between NQ from one protomer and heme *b* from the other protomer are labeled.

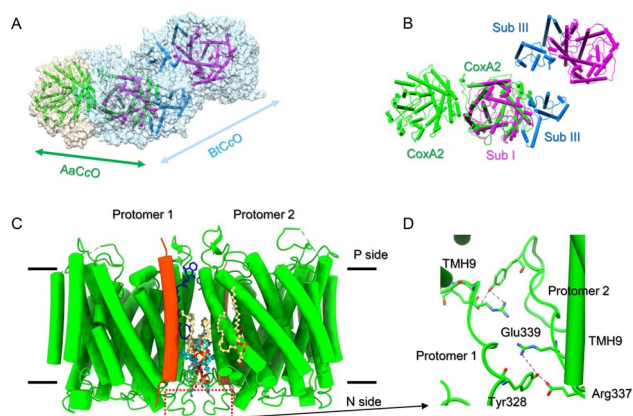


Figure 4. The dimer interfaces. A) Superimposed structures of AaCcO and BtCcO are illustrated as light tan and sky-blue transparent surfaces, respectively. AaCcO subunit I (CoxA2), BtCcO subunit I (Sub I), and subunit III (Sub III) are represented as cartoon and colored in green, purple, and light blue, respectively. The view is perpendicular to the membrane. B) The same view of (A) without showing the surfaces. C) The dimerization of AaCcO is mediated by both lipid–protein and protein–protein interactions. Lipid molecules PG, PE, and the quinone molecule NQ are colored in yellow, cyan and blue, respectively. CoxA2 is colored in green. The view is along the membrane. D) Zoomed-in view of protein–protein interactions at the dimer interface (C). Dotted lines indicate hydrogen bonds or electrostatic interactions.

found in the interface near the cytoplasmic side, which is occupied by many lipid molecules (Figure S4). Two PEs (phosphatidylethanolamine) and two PGs (phosphatidylglycerol) lipid molecules are identified in the cavity (Figure 4C). And four more PGs are found at the vicinity (Figure 4C). Interestingly, two quinol molecules (NQ) are found at the interface with the head group orientation towards the P-side (Figure 4C). Our subsequent lipidomics mass spectrometry analysis of co-purified lipids in the sample confirmed the exact chemical composition of PE and PG and the mass spectrometry analysis of native *A. aeolicus* membranes identified the native quinol molecule as VII-tetrahydromulti-prenyl-1,4-naphthoquinone^[25] (Figure S6).

The NQ binding site

We previously reported that AaCcO can use both reduced cytochrome *c* and quinol as electron donors.^[19] We originally hypothesized it would be caused by formation of a super-complex between AaCcO and complex III, providing additional quinol binding sites for its direct oxidation bypassing cytochrome *c*. However, our structural study of the *A. aeolicus* complex III^[20] does not support this hypothesis. Furthermore, our substantial image processing of the current purified sample does not suggest the existing of any potential supercomplex (Figure S2). Thus, oxidation of NQH₂ most likely occurs in the AaCcO itself, which can be proved by the dimeric structure of AaCcO and the existence of NQ molecules at the dimer interface (Figure S4). Each NQ molecule is deeply buried in the hydrophobic groove formed by subunits Ila and coxA2 (Figure 5A). Many hydrophobic residues interact with the NQ aliphatic chain, including Val36,

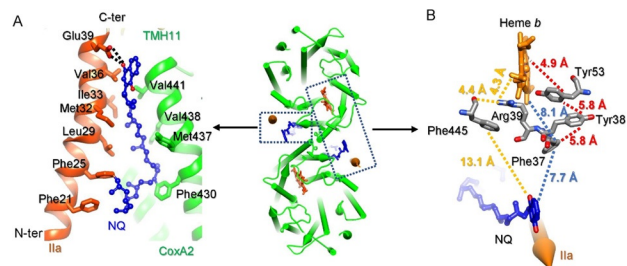


Figure 5. Potential quinol binding site of AaCcO. A) The quinone molecule NQ is buried between subunit Ila (orange) and TMH11 (green) of CoxA2. B) The distances between NQ of one protomer and the residues/heme *b* of another protomer are measured, showing potential electron transfer pathways from NQ to heme *b*.

Ile33, Met32, Leu29, Phe25, and Phe21 of Ila and Phe430, Met437, Val438, Val441 in TMH11 of CoxA2. In particular, one carbonyl oxygen of NQ is found to bind to Glu39 of subunit Ila (Figure 5A), a residue presents only in *A. aeolicus* (Figure S7A). A deprotonated Glu39 would form a strong hydrogen bond with the hydroxyl group of NQH₂ and accept one proton upon oxidation of NQH₂. To be noted, the NQ tail is buried inside one protomer while its carbonyl oxygen is proximal to heme *b* of another protomer (Figures 5A,B). The edge-to-edge distance between NQ and heme *b* is 15.0 Å. With this distance direct electron transfer is possible. In addition, the existence of several aromatic residues (Phe37, Tyr38, Tyr53, and Phe445) would be also possible involved in the electron transfer from NQH₂ to heme *b* (Figure 5B). This quinol binding pocket is similar to the menaquinol binding pocket in cytochrome *aa*₃-600 menaquinol oxidase from *Bacillus subtilis* (Figure S7B).^[24]

Only a K proton pathway exists in AaCcO

Based on the structure of a B-family CcO, the presence of three possible proton pathways, named K-, D-, and Q-pathways, were previously suggested.^[7] The residues for forming these pathways are usually conserved between different species with only a limited number of mutations. The K-pathway, named after its essential lysine residue Lys354, was identified previously.^[25] Structural superposition of the crystal structure of TtCcO and the cryo-EM structure of AaCcO reveals the presence of the K-pathway in AaCcO, except that at the start Glu516 in the subunit I of TtCcO is mutated to His515 in AaCcO (Figure 6A). In this pathway, protons can be transferred from His515 and Asp516 at the N side, via Ser252, Tyr237, Thr303, Tyr233, Ser300, and Tyr226 to the active site that is formed by the high spin heme *a*₃ and Cu_B. In the classical K-pathway, there is usually a conserved Glu of subunit II as a potential proton entry point,^[26] which is Glu15 in the subunit II of TtCcO and also conserved in AaCcO (Glu 5 of subunit II, Figure S8).

Structural superposition also reveals the potential D- and Q-pathway of AaCcO (Figures 6B,C). In the D-pathway of TtCcO, protons can be transferred from Glu17 on the cytoplasmic side, via Tyr91, Ser109, Ser155, Thr156, Ser197, Thr231, and several water molecules, to the heme *a*₃ active

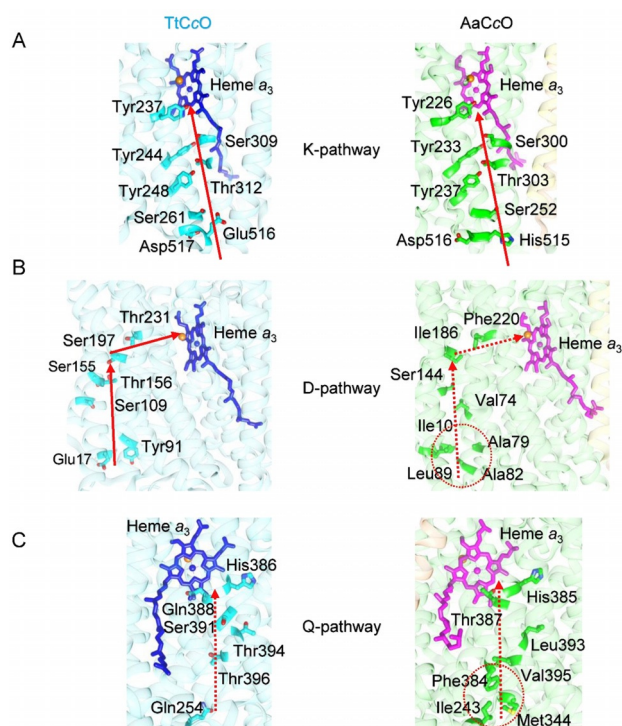


Figure 6. Only the K-pathway proton channel exists in AaCcO. A) The K-pathway channels of TtCcO (left) and AaCcO (right) are shown with the red arrow from the cytoplasmic side to the heme a_3 site. B) and C) The potential D-pathway (B) and Q-pathway (C) proton channels are blocked in AaCcO by various hydrophobic residues. The presumable directions of proton transfer are indicated by red dotted arrows.

site. However, in AaCcO, the entrance for protons is blocked by several hydrophobic residues, including Ala82, Leu89, Ala79, and Ile10. Furthermore, replacing hydrophilic residues to hydrophobic ones Val74, Ile186, and Phe220 does not allow proton transfer (Figure 6B). A similar situation was also found for the potential Q-pathway of AaCcO (Figure 6C). Thus, only the K-pathway does exist for proton transfer in AaCcO.

An unobstructed oxygen diffusion pathway in AaCcO

Based on the crystal structure of TtCcO, the presence of a Y-shaped oxygen diffusion pathway with two entry points was suggested^[7] (Figure 7A). Interestingly, in AaCcO one V-shaped potential oxygen diffusion pathway is observed (Figure 7B). There is only one entry point to this diffusion pathway, which starts at the middle of the membrane. In this pathway, O₂ enters a hydrophobic gate formed by Ile194, Ile193, Val138, and Leu135, turning at Phe220, Phe123, Val65, Ile66, and Trp121, then passes near Trp228, Val224, Val225, Phe220, Phe217, Trp218 to reach the heme a_3 active center (Figure 7B). Sequence alignment shows that most of the residues lining the putative oxygen pathway are conserved, except Phe113 in AaCcO (Figure S9). A structural superposition of TtCcO and AaCcO reveals that the oxygen entry point 2 might be blocked by Phe113 in AaCcO (Figure 7C).

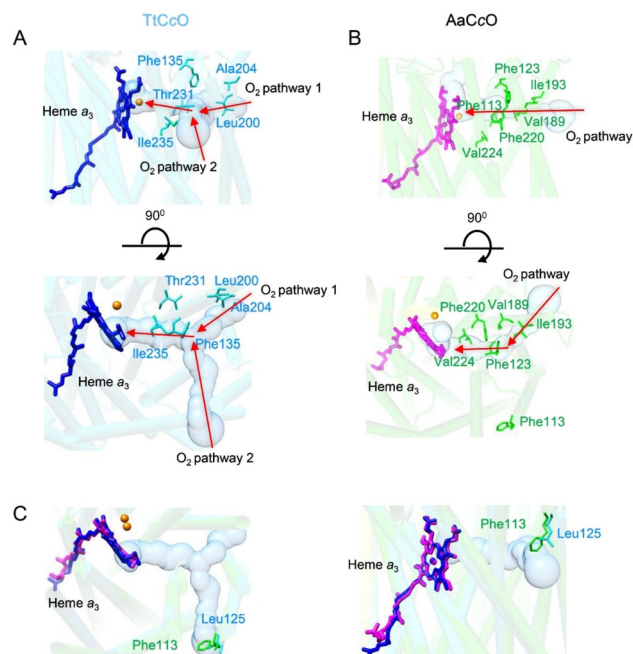


Figure 7. Oxygen channel in AaCcO. A) Y-shaped oxygen channel with two entry points in TtCcO is indicated by a solid surface. The entry point 1 starts near Ala204 and Leu200. B) V-shaped oxygen channel in AaCcO. The entry point 1 starts near Ile193 and Val189. C) The entry point 2 near Leu125 in TtCcO is blocked by Phe113 in AaCcO. Important residues are indicated and shown as sticks. The oxygen channels were calculated and predicted using MOLE2.^[27]

Discussion

The structures and functions of respiratory complexes from different species have been extensively studied in past years.^[28] Compared to conventional cytochrome *c* oxidases that use cytochrome *c* as the electron donor, AaCcO can directly oxidize quinol substrates besides cytochrome *c*.^[19] In the present study, we explored the high-resolution structure of AaCcO by single particle cryo-EM and got insights into the molecular mechanism of how AaCcO could use both cytochrome *c* and quinol as electron donors by discovering the existence of the native quinol molecules NQs bound at the dimeric interface. The edge-to-edge distance from NQ to heme *b* is close enough to enable a direct electron transfer from NQH₂ to the active binuclear center via heme *b*. The proximal aromatic residues between NQ and heme *b* would presumably enhance the rate of electron transfer. Subunit IIa was found to be important for NQ binding by ligation of the head group of NQ and the residue Glu39 of Subunit IIa presumably plays a role of stabilizing NQ during electron transfer. Notably, such electron transfer could only happen between NQ bound to one protomer and heme *b* of another protomer. Thus, the dimerization of AaCcO not only provides a new interface for NQ binding but also be necessary for direct electron transfer from NQ. Any regulation factor including thermal fluctuation that alters the formation of AaCcO dimer might affect its activity of direct NQH₂ oxidation, which could likely explain the low quinol oxidation activity measured previously.^[19]

Previous studies found BtCcO to form a homodimer in the crystals^[29] while it appears as a monomer in all supercomplex structures.^[30] A recent cryo-EM study discovered another intact 14th subunit (NDUFA4) of human cytochrome *c* oxidase, which is important to keep it in a monomeric active form but was absent in the previous dimeric less active form.^[31] At the same time, the structure of an active monomeric form of BtCcO was also determined by X-ray crystallography.^[32] Our present work does not rule out the existence of a supercomplex in *A. aeolicus*, which has been suggested in a previous study.^[33] However, the insensitivity of ubiquinol oxidation activity of the potential supercomplex to stigmatellin indicated that AaCcO itself has the activity of ubiquinol oxidation.^[19] After solving the structure of AaCcO, its ubiquinol oxidation activity could be only explained by its dimeric form. Furthermore, this dimeric form is different from that of all other reported CcO dimers. We also superimposed the dimeric structure of AaCcO into other reported respiratory supercomplexes from *Mycobacterium smegmatis* (*M. smegmatis*),^[34] *Saccharomyces cerevisiae* (*S. cerevisiae*)^[28e] and *Sus scrofa* (*S. scrofa*),^[35] and found the dimeric interface of AaCcO does not overlap the interface between complex III and complex IV in the supercomplexes from *M. smegmatis* and *S. scrofa* (Figure S10). Thus, to form a supercomplex, such dimeric form of AaCcO would not need to be broken.

Considering the hyperthermophilic growth environment of *A. aeolicus*, it would be interesting to investigate the unique structural features of its respiratory chain complex and understand the mechanism of structural adaptation suitable for hyperthermophilic environment. In our previous study of *A. aeolicus* complex III, we discovered an extra transmembrane helix of cyt. *c*₁ and several unique residues important for the thermostability of the complex.^[20] Interestingly, we also found that subunit I of AaCcO possesses two additional C-terminal transmembrane helices, THM13 and TMH14, in comparison with eukaryotic CcOs, or still one additional TMH when comparing with TtCcO, a thermophilic prokaryotic CcO. Thus, it might be possible that the presence of the extra TMHs of AaCcO enhances its thermal stability suitable for the hyperthermophilic growth conditions. In addition, the membrane-anchored cytochrome *c*₅₅₅ might bind to this TMH14, as proposed for the *aa*₃-type CcO from *P. denitrificans*.^[36]

Based on the crystal structure of TtCcO, three proton transfer pathways (K, D, and Q) were proposed.^[7] Mutations of critical residues on D-pathway (S109A) and Q-pathway (T396V) showed little influence on the enzymatic activity.^[15,37] Structural superposition of TtCcO and AaCcO reveals that the D- and Q-proton pathways in AaCcO are both blocked by multiple hydrophobic residues. Therefore, even if the D- and Q-proton pathways in TtCcO were active, the same pathways in AaCcO should be closed and inactive. Only the K-pathway appears to be present in AaCcO. Besides the proton transfer pathway, the potential oxygen diffusion channel of AaCcO also varies in comparison with that of TtCcO. Along with conserved oxygen channels being suggested for CcOs from *Rhodobacter sphaeroides*,^[38] *P. denitrificans*^[39] and *B. taurus*,^[9b] a Y-shaped oxygen channel was also

reported in TtCcO, suggesting that there are two entry points for oxygen. However, structural superposition of AaCcO and TtCcO suggest that only one oxygen diffusion channel exists and forms a V-shape in AaCcO. The second oxygen entry point 2 found in TtCcO is blocked by residue Phe113 in AaCcO at the equivalent position. The larger the void in a protein, the smaller is its stability.^[40] The adapted structure of AaCcO with only the K proton pathway present and the V-shaped unobstructed oxygen channel with more hydrophobic residues blocking one entry appears to be evolutionary advantageous to keep the balance between its enzymatic activity and structural stability in the hyperthermophilic environment.

Conclusion

In summary, we solved the 3.4 Å structure of cytochrome *c* oxidase from the hyperthermophilic bacterium *Aquifex aeolicus*, revealed the molecular mechanism that this oxidase uses both cytochrome *c* and quinol as electron donors, made structural insights into its thermal stability, and suggested an evolutionary adaptation of this oxidase to keep the balance between its enzymatic activity and structural stability for the hyperthermophilic growth condition. These results provide structural basis for molecular mechanism and the evolutionary significance of cytochrome *c* oxidases in an extreme thermal environment.

Data and materials availability

The atomic coordinates of the cytochrome *c* oxidase of *Aquifex aeolicus* reported in this paper have been deposited in Worldwide Protein Data Bank (PDB) (<http://www.rcsb.org>) with the accession codes 7DEG. The corresponding maps have been deposited in the Electron Microscope Data Bank (EMDB) (<http://emdatbank.org>) with the accession codes EMD-30657.

Acknowledgements

We thank Ping Shan, Ruigang Su and Mengyue Lou (F.S. lab) for their assistance in lab management. The materials were prepared at the Max Planck Institute of Biophysics, whereas the cryo-EM work was performed at the Center for Biological Imaging (CBI, <http://cbi.ibp.ac.cn>), Core Facilities for Protein Science at the Institute of Biophysics (IBP), Chinese Academy of Sciences (CAS). We would also like to thank B. Zhu, X. Huang, X. Li, T. Niu, G. Ji, D. Fan and other staff members from CBI for their help in data collection. We thank Zhensheng Xie from Lab of Proteomics, Core Facilities for protein Science, IBP, CAS for her help on LC-MS analysis. We thank Ulrich Ermler for his advice on data analysis. This work was equally supported by grants from Strategic Priority Research Program of Chinese Academy of Sciences (XDB37040102), the National Key Research and Development Program of China (2017YFA0504700) and National

Natural Science Foundation of China (31830020). This work was also supported by grants from Max-Planck-Gesellschaft and the Deutsche Forschungsgemeinschaft (Cluster of Excellence Macromolecular Complexes, Frankfurt) and the Ministry of Science and Technology of China (2018YFA0901102 and 2019YFA0904101). Open access funding enabled and organized by Projekt DEAL.

Conflict of interest

The authors declare no conflict of interest.

Keywords: cytochrome *c* oxidase · dimerization · enzyme catalysis · naphthoquinone · protein structures

- [1] a) H. Michel, J. Behr, A. Harrenga, A. Kannt, *Annu. Rev. Biophys. Biomol. Struct.* **1998**, *27*, 329–356; b) H. Michel, *Proc. Natl. Acad. Sci. USA* **1998**, *95*, 12819–12824.
- [2] a) G. T. Babcock, M. Wikstrom, *Nature* **1992**, *356*, 301–309; b) M. W. Calhoun, J. W. Thomas, R. B. Gennis, *Trends Biochem. Sci.* **1994**, *19*, 325–330; c) S. Ferguson-Miller, G. T. Babcock, *Chem. Rev.* **1996**, *96*, 2889–2907.
- [3] J. A. García-Horsman, B. Barquera, J. Rumbley, J. X. Ma, R. B. Gennis, *J. Bacteriol.* **1994**, *176*, 5587–5600.
- [4] G. N. Green, H. Fang, R. J. Lin, G. Newton, M. Mather, C. D. Georgiou, R. B. Gennis, *J. Biol. Chem.* **1988**, *263*, 13138–13143.
- [5] a) M. M. Pereira, F. L. Sousa, A. F. Verissimo, M. Teixeira, *Biochim. Biophys. Acta Bioenerg.* **2008**, *1777*, S66–S66; b) J. Hemp, R. B. Gennis, *Results Probl. Cell Differ.* **2008**, *45*, 1–31; c) M. M. Pereira, M. Santana, M. Teixeira, *Biochim. Biophys. Acta Bioenerg.* **2001**, *1505*, 185–208.
- [6] E. Balsa, R. Marco, E. Pereles-Clemente, R. Szklarczyk, E. Calvo, M. O. Landazuri, J. A. Enriquez, *Cell Metab.* **2012**, *16*, 378–386.
- [7] T. Soulimane, G. Buse, G. P. Bourenkov, H. D. Bartunik, R. Huber, M. E. Than, *EMBO J.* **2000**, *19*, 1766–1776.
- [8] B. C. Hill, *J. Biol. Chem.* **1994**, *269*, 2419–2425.
- [9] a) T. Tsukihara, H. Aoyama, E. Yamashita, T. Tomizaki, H. Yamaguchi, K. Shinzawa-Itoh, R. Nakashima, R. Yaono, S. Yoshikawa, *Science* **1995**, *269*, 1069–1074; b) T. Tsukihara, H. Aoyama, E. Yamashita, T. Tomizaki, H. Yamaguchi, K. Shinzawa-Itoh, R. Nakashima, R. Yaono, S. Yoshikawa, *Science* **1996**, *272*, 1136–1144.
- [10] J. Abramson, S. Riistama, G. Larsson, A. Jasaitis, M. Svensson-Ek, L. Laakkonen, A. Puustinen, S. Iwata, M. Wikstrom, *Nat. Struct. Biol.* **2000**, *7*, 910–917.
- [11] a) H. Witt, F. Malatesta, F. Nicoletti, M. Brunori, B. Ludwig, *J. Biol. Chem.* **1998**, *273*, 5132–5136; b) H. Witt, F. Malatesta, F. Nicoletti, M. Brunori, B. Ludwig, *Eur. J. Biochem.* **1998**, *251*, 367–373.
- [12] A. Puustinen, M. Finel, T. Haltia, R. B. Gennis, M. Wikstrom, *Biochemistry* **1991**, *30*, 3936–3942.
- [13] J. A. Lyons, D. Aragao, O. Slattery, A. V. Pislakov, T. Soulimane, M. Caffrey, *Nature* **2012**, *487*, 514–518.
- [14] T. Tiefenbrunn, W. Liu, Y. Chen, V. Katritch, C. D. Stout, J. A. Fee, V. Cherezov, *Plos One* **2011**, *6*, e22348.
- [15] H. Y. Chang, J. Hemp, Y. Chen, J. A. Fee, R. B. Gennis, *Proc. Natl. Acad. Sci. USA* **2009**, *106*, 16169–16173.
- [16] V. Rauhamäki, M. Wikstrom, *Biochim. Biophys. Acta Bioenerg.* **2014**, *1837*, 999–1003.
- [17] A. Kannt, T. Soulimane, G. Buse, A. Becker, E. Bamberg, H. Michel, *FEBS Lett.* **1998**, *434*, 17–22.
- [18] M. M. Pereira, M. Santana, C. M. Soares, J. Mendes, J. N. Carita, A. S. Fernandes, M. Saraste, M. A. Carrondo, M. Teixeira, *Biochim. Biophys. Acta Bioenerg.* **1999**, *1413*, 1–13.
- [19] Y. Gao, B. Meyer, L. Sokolova, K. Zwicker, M. Karas, B. Brutschy, G. H. Peng, H. Michel, *Proc. Natl. Acad. Sci. USA* **2012**, *109*, 3275–3280.
- [20] G. L. Zhu, H. Zeng, S. B. Zhang, J. Juli, X. Y. Pang, J. Hoffmann, Y. Zhang, N. Morgner, Y. Zhu, G. H. Peng, H. Michel, F. Sun, *Angew. Chem. Int. Ed.* **2020**, *59*, 343–351; *Angew. Chem.* **2020**, *132*, 351–359.
- [21] a) S. H. W. Scheres, *J. Struct. Biol.* **2012**, *180*, 519–530; b) D. Kimanius, B. O. Forsberg, S. H. Scheres, E. Lindahl, *eLife* **2016**, *5*, e18722.
- [22] M. W. Adams, R. M. Kelly, *Trends Biotechnol.* **1998**, *16*, 329–332.
- [23] P. Infossi, E. Lojou, J. P. Chauvin, G. Herbette, M. Brugna, M. T. Giudici-Ortoni, *Int. J. Hydrogen Energy* **2010**, *35*, 10778–10789.
- [24] J. Xu, Z. Ding, B. Liu, S. M. Yi, J. Li, Z. Zhang, Y. Liu, J. Li, L. Liu, A. Zhou, R. B. Gennis, J. Zhu, *Proc. Natl. Acad. Sci. USA* **2020**, *117*, 872–876.
- [25] J. W. Thomas, A. Puustinen, J. O. Alben, R. B. Gennis, M. Wikstrom, *Biochemistry* **1993**, *32*, 10923–10928.
- [26] a) J. Koepke, E. Olkhova, H. Angerer, H. Muller, G. H. Peng, H. Michel, *Biochim. Biophys. Acta Bioenerg.* **2009**, *1787*, 635–645; b) M. Brändén, F. Tomson, R. B. Gennis, P. Brzezinski, *Biochemistry* **2002**, *41*, 10794–10798; c) O. M. H. Richter, K. L. Durr, A. Kannt, B. Ludwig, F. M. Scandurr, A. Giuffre, P. Sarti, P. Hellwig, *FEBS J.* **2005**, *272*, 404–412.
- [27] D. Sehnal, R. S. Vrekovaa, K. Berka, L. Pravda, V. Navratilova, P. Banas, C. M. Ionescu, M. Otyepka, J. Koca, *J. Cheminf.* **2013**, *5*, 39.
- [28] a) H. Gong, J. Li, A. Xu, Y. Tang, W. Ji, R. Gao, S. Wang, L. Yu, C. Tian, J. Li, H. Y. Yen, S. Man Lam, G. Shui, X. Yang, Y. Sun, X. Li, M. Jia, C. Yang, B. Jiang, Z. Lou, C. V. Robinson, L. L. Wong, L. W. Guddat, F. Sun, Q. Wang, Z. Rao, *Science* **2018**, *362*, eaat8923; b) R. Guo, S. Zong, M. Wu, J. Gu, M. Yang, *Cell* **2017**, *170*, 1247–1257; c) S. Rathore, J. Berndtsson, L. Marin-Buera, J. Conrad, M. Carroni, P. Brzezinski, M. Ott, *Nat. Struct. Mol. Biol.* **2019**, *26*, 50–57; d) H. Yu, C. H. Wu, G. J. Schut, D. K. Haja, G. Zhao, J. W. Peters, M. W. W. Adams, H. Li, *Cell* **2018**, *173*, 1636–1649; e) A. M. Hartley, N. Lukoyanova, Y. Zhang, A. Cabrera-Orefice, S. Arnold, B. Meunier, N. Pinotsis, A. Marechal, *Nat. Struct. Mol. Biol.* **2019**, *26*, 78–83.
- [29] S. Yoshikawa, K. Shinzawa-Itoh, R. Nakashima, R. Yaono, E. Yamashita, N. Inoue, M. Yao, M. J. Fei, C. P. Libeu, T. Mizushima, H. Yamaguchi, T. Tomizaki, T. Tsukihara, *Science* **1998**, *280*, 1723–1729.
- [30] a) J. Gu, M. Wu, R. Guo, K. Yan, J. Lei, N. Gao, M. Yang, *Nature* **2016**, *537*, 639–643; b) R. Guo, J. Gu, M. Wu, M. Yang, *Protein Cell* **2016**, *7*, 854–865; c) J. A. Letts, K. Fiedorczuk, L. A. Sazanov, *Nature* **2016**, *537*, 644.
- [31] S. Zong, M. Wu, J. Gu, T. Liu, R. Guo, M. Yang, *Cell Res.* **2018**, *28*, 1026–1034.
- [32] K. Shinzawa-Itoh, T. Sugimura, T. Misaki, Y. Tadehara, S. Yamamoto, M. Hanada, N. Yano, T. Nakagawa, S. Uene, T. Yamada, H. Aoyama, E. Yamashita, T. Tsukihara, S. Yoshikawa, K. Muramoto, *Proc. Natl. Acad. Sci. USA* **2019**, *116*, 19945–19951.
- [33] L. Prunetti, P. Infossi, M. Brugna, C. Ebel, M. T. Giudici-Ortoni, M. Guiral, *J. Biol. Chem.* **2010**, *285*, 41815–41826.
- [34] B. Wiseman, R. G. Nitharwal, O. Fedotovskaya, J. Schafer, H. Guo, Q. Kuang, S. Benlekkir, D. Sjostrand, P. Adelroth, J. L. Rubinstein, P. Brzezinski, M. Hoggom, *Nat. Struct. Mol. Biol.* **2018**, *25*, 1128–1136.
- [35] M. Wu, J. Gu, R. Guo, Y. Huang, M. Yang, *Cell* **2016**, *167*, 1598–1609.

- [36] J. W. de Gier, M. Schepper, W. N. Reijnders, S. J. van Dyck, D. J. Slotboom, A. Warne, M. Saraste, K. Krab, M. Finel, A. H. Stouthamer, R. J. van Spanning, J. van der Oost, *Mol. Microbiol.* **1996**, *20*, 1247–1260.
- [37] H. Y. Chang, S. K. Choi, A. S. Vakkasoglu, Y. Chen, J. Hemp, J. A. Fee, R. B. Gennis, *Proc. Natl. Acad. Sci. USA* **2012**, *109*, 5259–5264.
- [38] M. Svensson-Ek, J. Abramson, G. Larsson, S. Tornroth, P. Brzezinski, S. Iwata, *J. Mol. Biol.* **2002**, *321*, 329–339.
- [39] S. Iwata, C. Ostermeier, B. Ludwig, H. Michel, *Nature* **1995**, *376*, 660–669.
- [40] B. Lee, *Protein Sci.* **1993**, *2*, 733–738.

Manuscript received: December 18, 2020
Accepted manuscript online: March 4, 2021
Version of record online: May 6, 2021